

Electronic Supplementary Information (ESI)

Controllable Conversion of Prussian blue@yeast bio-template into 3D Cage-like Magnetic Fe₃O₄@N-doped Carbon Absorbent and its Cohesive Regeneration by Persulfate Activation

Si Chen ^{a, b}, Bo Bai ^{*, b, c, d}, Yunhua He ^{a, b}, Na Hu ^{c, d}, Honglun Wang ^{c, d}, Yourui Suo ^{c, d}

^a Key Laboratory of Subsurface Hydrology and Ecological Effects in Arid Region of the Ministry of Education, Chang'an University, No. 126 Yanta Road, Xi'an 710054, Shaanxi, China,

^b College of Environmental Science and Engineering, Chang'an University, Xi'an, 710054, P.R. China;

^c Key Laboratory of Tibetan Medicine Research, Northwest Institute of Plateau Biology, Chinese Academy of Sciences, Xining, 810008, China;

^d Qinghai Provincial Key Laboratory of Tibetan Medicine Research, Xining, 810001, P.R. China)

* Corresponding author

Email address: baibochina@163.com

Tel: +86 29 82339052

Fax: +86 29 82339961

Contents

Fig. S1 FE-SEM images of (a-b) Fe₃O₄@C (1:0.05); (c-d) Fe₃O₄@C (1:0.22).

Fig. S2 EDS analysis of (a) Fe₃O₄@C (1:0.05) and (b) Fe₃O₄@C (1:0.22).

Fig. S3 EDS analysis of N-doped Fe₃O₄@C (1:0.11) and the corresponding mapping images.

Fig. S4 XRD patterns of PB@yeast bio-templates.

Fig. S5 Linear fits of experimental data for (a) Langmuir isotherm model; (b) Freundlich isotherm model; (c) pseudo-first kinetic model; (d) pseudo-second kinetic model.

Fig. S6 Linear fits at different temperature for (a) Langmuir isotherm model and (b) Freundlich isotherm model.

Table S1 Comparison of maximum adsorption capacities of adsorbents for RhB in previous literatures

Table S2 Kinetic parameters for RhB adsorption at different initial concentration

Table S3 Adsorption isotherm parameters for RhB adsorption at different temperatures

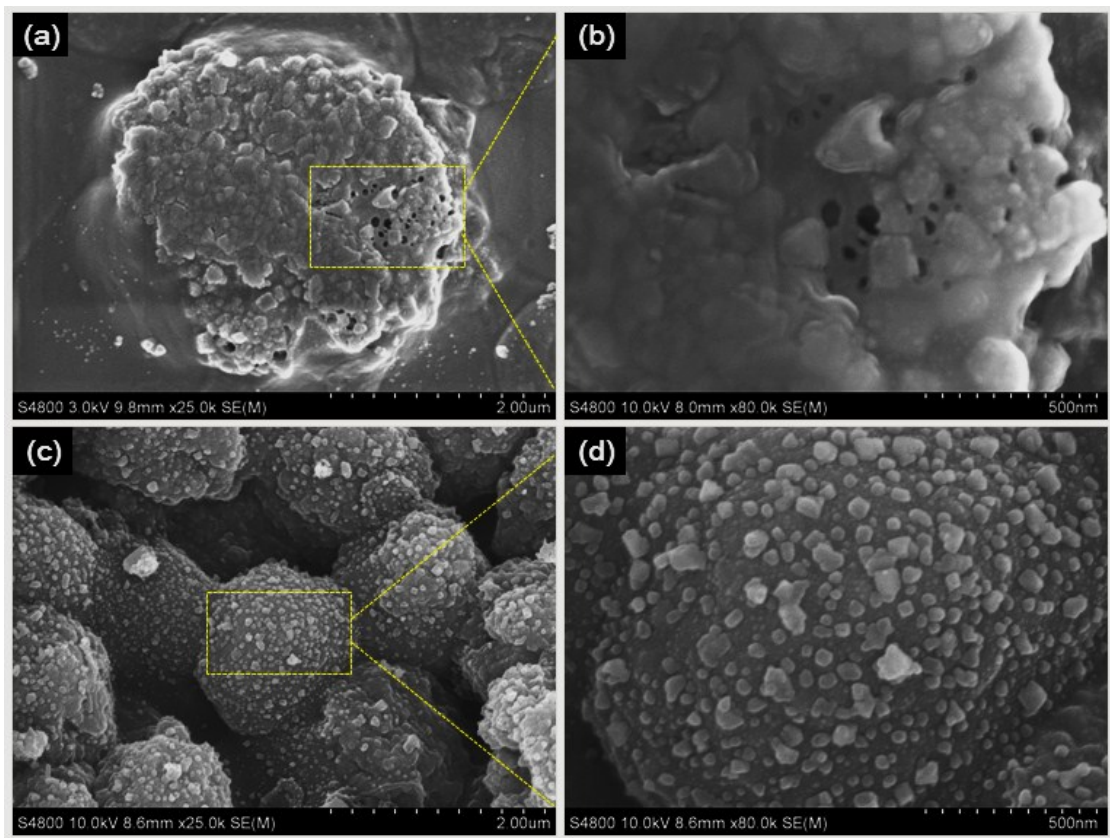


Fig. S1 FE-SEM images of (a-b) Fe_3O_4 @C (1:0.05) and (c-d) Fe_3O_4 @C (1:0.22).

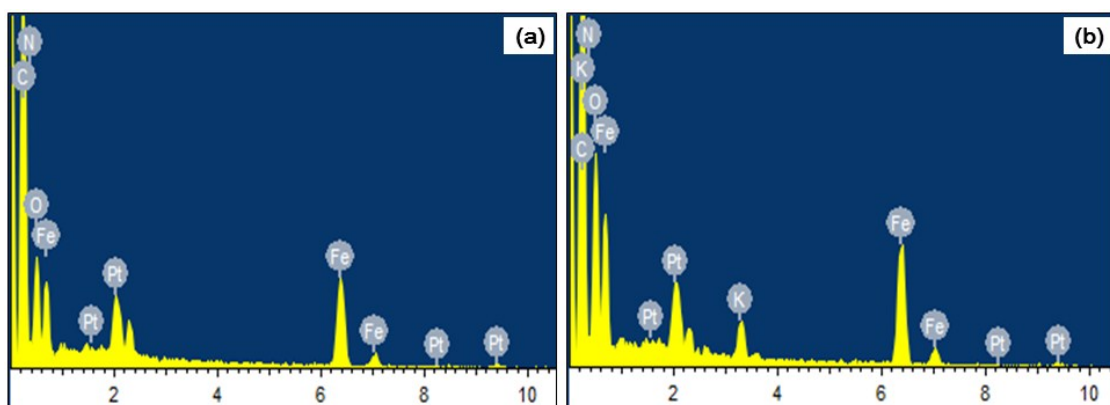


Fig. S2 EDS analysis of (a) Fe_3O_4 @C (1:0.05) and (b) Fe_3O_4 @C (1:0.22).

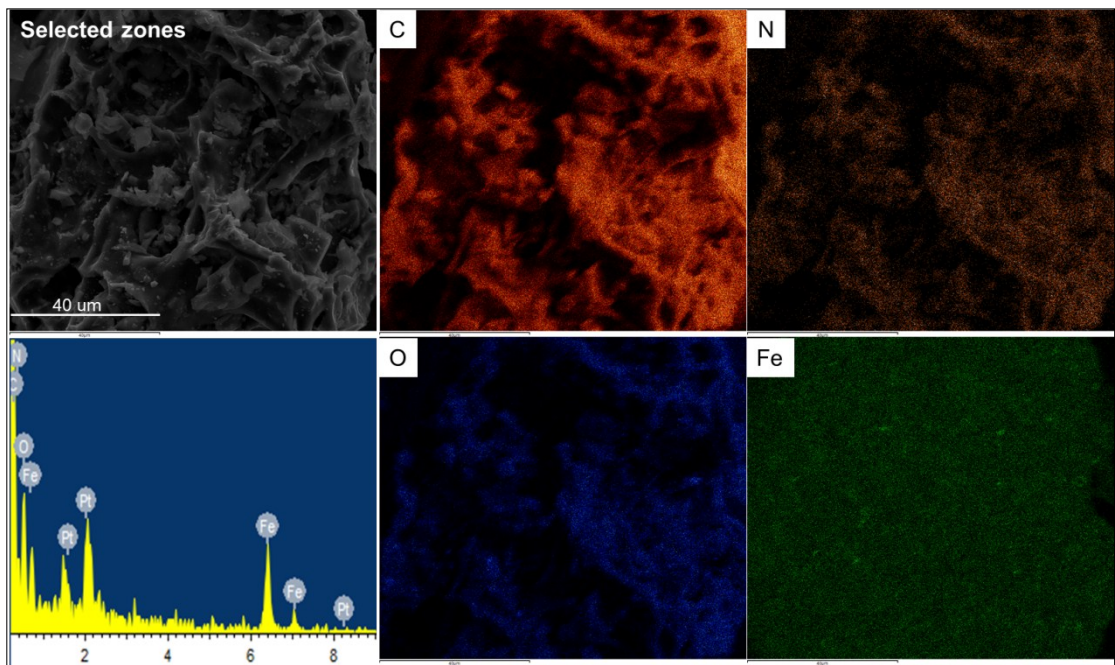


Fig. S3 EDS analysis of N-doped $\text{Fe}_3\text{O}_4@\text{C}$ (1:0.11) and the corresponding mapping images.

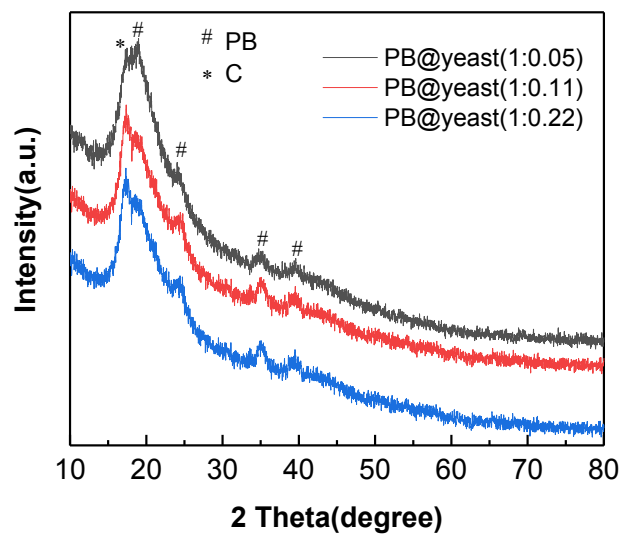


Fig. S4 XRD patterns of PB@yeast bio-templates.

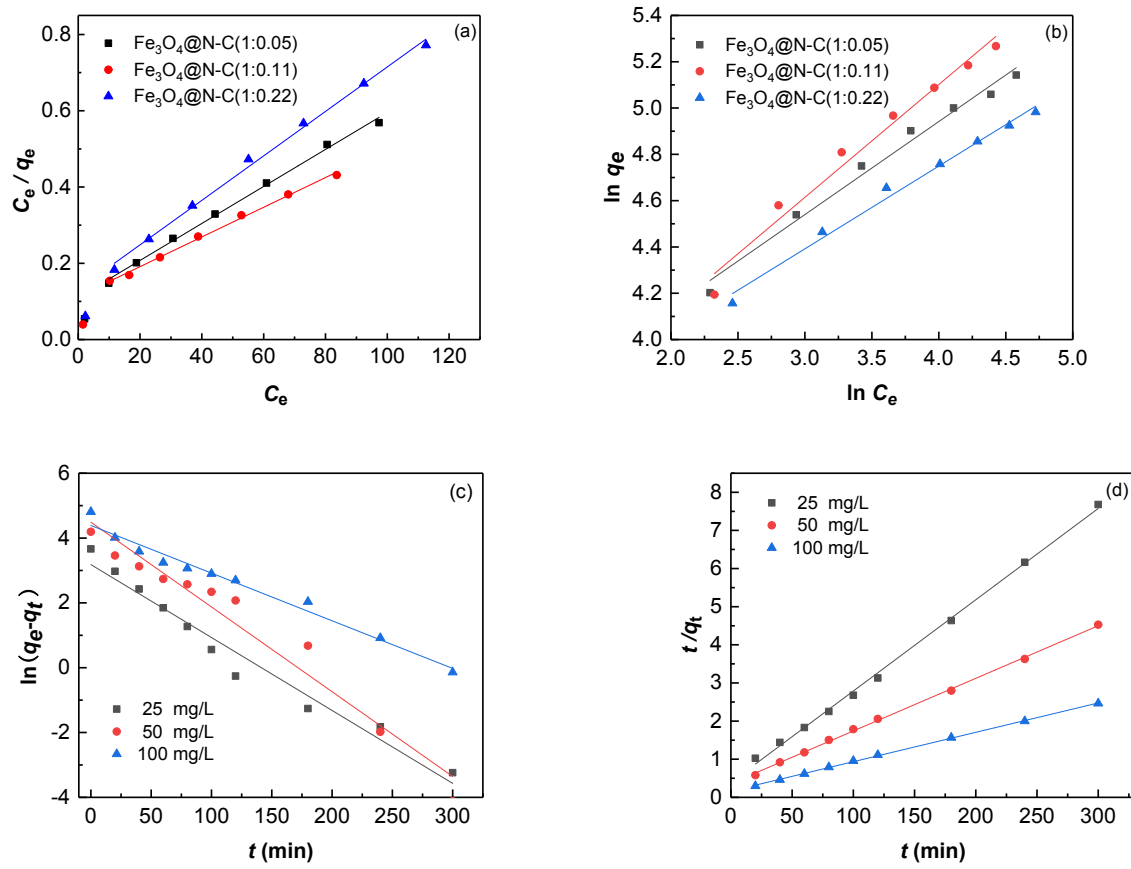


Fig. S5 Linear fits of experimental data for (a) Langmuir isotherm model; (b) Freundlich isotherm model; (c) pseudo-first kinetic model; (d) pseudo-second kinetic model.

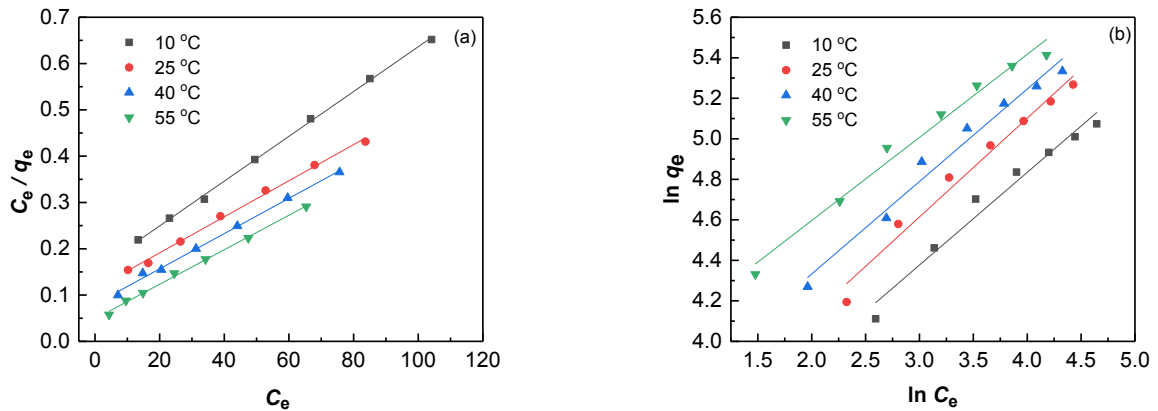


Fig. S6 Linear fits at different temperature for (a) Langmuir isotherm model and (b) Freundlich isotherm model.

Table S1 Comparison of maximum adsorption capacities of adsorbents for RhB in previous literatures

Adsorbent	T (°C)	pH	q_{\max} (mg·g ⁻¹)	References
gelatin/activated carbon composite beads(GE/AC)	60	4.0	256.41	1
Fe ₃ O ₄ /RGO	60	5.3	142.86	2
In-MOF@GO-2	25	6.0	267	3
iron-pillared bentonite (Fe-Ben)	25	5.0	98.6	4
carbonaceous adsorbent (TPC)prepared from Thespusia populinia bark	60	7.0	77.18	5
Fe ₃ O ₄ @N-C (1:0.05)	25	6.0	206.19	This study
Fe ₃ O ₄ @N-C (1:0.11)	25	6.0	257.06	This study
Fe ₃ O ₄ @N-C (1:0.22)	25	6.0	171.53	This study

Table S2 Kinetic parameters for RhB adsorption at different initial concentration

Kinetic models	Parameters	C_0 of RhB ($\text{mg}\cdot\text{L}^{-1}$)		
		25	50	100
Pseudo-first-order	$q_{e,\text{exp}}$ ($\text{mg}\cdot\text{g}^{-1}$)	39.06	66.28	122.61
	$q_{e,\text{cal}}$ ($\text{mg}\cdot\text{g}^{-1}$)	8.65	12.20	11.93
	k_1 (min^{-1})	0.0225	0.0262	0.0147
	R^2	0.9643	0.9515	0.9747
pseudo-second-order	$q_{e,\text{cal}}$ ($\text{mg}\cdot\text{g}^{-1}$)	41.77	72.46	129.87
	$k_2 \times 10^{-3}$ ($\text{g}\cdot\text{mg}^{-1}\text{min}^{-1}$)	1.4537	0.5262	0.3576
	R^2	0.9977	0.9989	0.9993
	k_{1d} ($\text{mg}\cdot\text{g}^{-1}\text{min}^{-0.5}$)	4.6083	5.6125	10.3763
intra-particle diffusion	R^2	0.9788	0.9968	0.9841
	k_{2d} ($\text{mg}\cdot\text{g}^{-1}\text{min}^{-0.5}$)	1.7468	2.3845	3.2649
	R^2	0.9605	0.9960	0.9961
	k_{3d} ($\text{mg}\cdot\text{g}^{-1}\text{min}^{-0.5}$)	0.0959	0.1495	0.9077
	R^2	0.8401	0.5680	0.9273

Table S3 Adsorption isotherm parameters for RhB adsorption at different temperatures

T (°C)	Langmuir Model			Freundlich Model			
	q_{\max} (mg·g ⁻¹)	K_L (L ·g ⁻¹)	R^2	R_L	1/n	K_F (L ·g ⁻¹)	R^2
10	206.61	0.0317	0.9988	0.14-0.39	0.4575	8.1669	0.9709
25	257.06	0.0343	0.9965	0.13-0.37	0.4874	8.5676	0.9778
40	262.46	0.0437	0.9954	0.10-0.30	0.4564	9.2963	0.9772
55	268.10	0.0764	0.9965	0.06-0.21	0.4101	10.265	0.9825

References

- 1 F. Hayeeye, M. Sattar, W. Chinpa and O. Sirichote, *Colloid Surface A*, 2017,**513**, 259-266.
- 2 Y. Qin, M. Long, B. Tan and B. Zhou, *Nano-Micro Lett.*, 2014, **6**, 125-135.
- 3 C. Yang, S. Wu, J. Cheng and Y. Chen, *J. Alloy Compd.*, 2016,**687**, 804-812.
- 4 M.F. Hou, C.X. Ma, W.D. Zhang, X.Y. Tang, Y.N. Fan and H.F. Wan, *J. Hazard. Mater.* 2011,**186**, 1118-1123.
- 5 M. Hema and S. Arivoli, *Indian J. Chem. Technol.* 2009, **16**, 38-45.